[CANCER RESEARCH 63, 3886–3890, July 15, 2003]

Advances in Brief

Nkx3.1; Pten Mutant Mice Develop Invasive Prostate Adenocarcinoma and Lymph Node Metastases[1]

Cory Abate-Shen,[2] Whitney A. Banach-Petrosky,[3] Xiaohui Sun,[3] Kyriakos D. Economides, Nishita Desai, Jeffery P. Gregg, Alexander D. Borowsky, Robert D. Cardiff, and Michael M. Shen[2]

Center for Advanced Biotechnology and Medicine [C. A-S., W. A. B-P., X. S., K. D. E., N. D., M. M. S.], Departments of Medicine [C. A-S., W. A. B-P., X. S., K. D. E.], Neuroscience and Cell Biology [C. A-S., W. A. B-P., X. S., K. D. E.], and Pediatrics [N. D., M. M. S.], and The Cancer Institute of New Jersey [C. A-S., M. M. S.], University of Medicine and Dentistry, New Jersey-Robert Wood Johnson Medical School, Piscataway, New Jersey 08854, and Department of Medical Pathology and Center for Comparative Medicine, University of California, Davis, California [J. P. G., A. D. B., R. D. C.]

Abstract

Recent studies have shown that several loss-of-function mouse models of prostate carcinogenesis can develop a spectrum of precancerous lesions that resemble human prostatic intraepithelial neoplasia (PIN). Here, we have investigated the malignant potential of the high-grade PIN lesions that form in *Nkx3.1*$^{+/-}$; *Pten*$^{+/-}$ compound mutant mice and demonstrate their neoplastic progression in a serial transplantation/tissue recombination assay. Furthermore, we find that a majority of *Nkx3.1*$^{+/-}$; *Pten*$^{+/-}$ mice greater than 1 year of age develop invasive adenocarcinoma, which is frequently accompanied by metastases to lymph nodes. Finally, we observe androgen independence of high-grade PIN lesions after androgen ablation of *Nkx3.1*$^{+/-}$; *Pten*$^{+/-}$ mice. We conclude that *Nkx3.1*$^{+/-}$; *Pten*$^{+/-}$ mice recapitulate key features of advanced prostate cancer and represent a useful model for investigating associated molecular mechanisms and for evaluating therapeutic approaches.

Introduction

Adenocarcinoma of the prostate undergoes a characteristic progression from precursor lesions, termed PIN[4], to invasive carcinoma and ultimately metastases (reviewed in Refs. 1–3). Although the precise etiology of the disease is unknown, the most significant single risk factor for prostate carcinogenesis appears to be aging; thus, men as young as in their 20s display PIN lesions, whereas clinically detectable prostate cancer is usually not manifest until the sixth decade or later. If detected at early stages when locally confined, prostate cancer can often be eradicated using surgery or radiation therapy; however, metastatic disease can only be treated effectively by androgen ablation therapy, which ultimately leads to the recurrence of a highly aggressive, androgen-independent cancer. In this regard, the generation of mouse models of advanced stages of prostate cancer, particularly the transition to androgen independence and metastasis, may be useful for investigation of the underlying molecular mechanisms, as well as for preclinical studies of potential therapeutics.

We have been developing mouse models of prostate carcinogenesis that are based on the loss-of-function of genes known to be important for human prostate cancer, including *NKX3.1* and *PTEN* (reviewed in Ref. 4). *NKX3.1* is a homeobox gene that displays prostate-specific expression and maps to a critical region of chromosome 8p21, which undergoes allelic deletion in ~80% of prostatic neoplasias, and has been implicated in prostate cancer initiation because it is also prevalent in PIN lesions (reviewed in Ref. 5). Although the remaining *NKX3.1* allele does not appear to be mutated in prostate cancer (6), it instead undergoes epigenetic inactivation through loss of protein expression (7). Targeted deletion of *Nkx3.1* in mice leads to formation of PIN as a consequence of aging in both homozygous and heterozygous mutants (8, 9). Notably, the occurrence of PIN in *Nkx3.1* heterozygous mice is coincident with loss of Nkx3.1 protein expression (10), analogous to human cancer. Thus, *Nkx3.1* heterozygous and homozygous mutant mice recapitulate many features of early stages of prostate carcinogenesis in humans.

Another central regulator of human prostate carcinogenesis is the *PTEN* tumor suppressor gene, which maps to 10q23, a chromosomal region that is frequently lost at more advanced stages of prostate carcinogenesis (reviewed in Ref. 5). In addition, loss of *PTEN* expression is well correlated with increasing Gleason score and advanced histopathology in human prostate cancer (11). Because *PTEN* encodes a lipid phosphatase that is a negative regulator of the phosphatidylinositol 3′-kinase-AKT pathway, loss-of-function for *PTEN* results in inappropriate activation of AKT and consequent antiapoptotic effects in prostate cancer cells (reviewed in Refs. 12, 13). In mice, *Pten* loss-of-function mutations result in homozygous embryonic lethality, whereas heterozygotes display dysplasia and/or carcinoma of many tissues, including prostate (reviewed in Ref. 12; also see Ref. 14).

In previous studies, we have found that loss-of-function of *Nkx3.1* and *Pten* cooperate in prostate carcinogenesis in mutant mice, resulting in high-grade PIN/carcinoma *in situ* in compound heterozygotes by 6 months of age (10). We have now investigated the malignant potential of these preinvasive lesions in *Nkx3.1; Pten* compound mutants using a serial tissue recombination/transplantation assay or as a consequence of aging. We find that the resulting cancer lesions recapitulate key features of human prostate adenocarcinoma, including invasiveness, androgen independence, and the ability to metastasize. These observations indicate that *Nkx3.1; Pten* mutant mice represent models of invasive prostate adenocarcinoma and display at least some aspects of advanced prostate cancer.

Materials and Methods

Mice carrying null alleles of *Nkx3.1* and/or *Pten* have been described previously (8–10, 15). Analyses were performed on a hybrid 129/SvImJ-C57BL/6J strain background using virgin males. The primary histological analyses were performed on formalin-fixed tissues on a nonblinded basis by

Received 5/8/03; accepted 5/28/03.

The costs of publication of this article were defrayed in part by the payment of page charges. This article must therefore be hereby marked *advertisement* in accordance with 18 U.S.C. Section 1734 solely to indicate this fact.

[1] This work was supported by National Cancer Institute Grants CA76501 (to C. A-S.) and CA89140 (to R. D. C.), National Institutes of Diabetes, Digestive and Kidney Diseases Grant DK60887 (to M. M. S.) and the Department of Defense Prostate Cancer Research Program Grant DAMD17-03-1-0126 (to C. A-S.). C. A-S., M. M. S., and R. D. C. are investigators of the Mouse Models of Human Cancer Consortium (supported by Grant CA84294). The human tissue core at the Cancer Center, University of California, Davis, is supported by National Cancer Institute Grant CA93373.

[2] To whom requests for reprints should be addressed, at CABM, 679 Hoes Lane, Piscataway, NJ 08854. Phone: (732) 235-5161; Fax: (732) 235-5789; E-mail: abate@cabm.rutgers.edu (C. A-S.) or Phone: (732) 235-5645; Fax: (732) 235-5373; E-mail: mshen@cabm.rutgers.edu (M. M. S.).

[3] These authors contributed equally to this work.

[4] The abbreviations used are: prostatic intraepithelial neoplasia; AR, androgen receptor; *p*-Akt, phospho-Akt; DLP, dorsolateral lobe of the prostate.

two pathologists (R. D. C. and A. D. B.) and a blinded basis by C. A-S. Immunohistochemistry was performed on formalin-fixed tissues using previously described antisera (10); the anti-AR antisera was from Affinity Bioreagents (Golden, CO), and apoptosis was measured using an *in situ* cell death kit from Roche (Indianapolis, IN).

Serial transplantation of tissue recombinants was performed as described previously (9). Briefly, a segment of prostatic epithelium (~300 μm) from *Nkx3.1*$^{+/-}$; *Pten*$^{+/-}$ mutants (6–10 months) or age-matched, wild-type controls was combined with mouse or rat embryonic urogenital sinus mesenchyme and grown under the kidney capsule of nude male hosts for 1–2 months. After recovery, a segment of the tissue recombinants (~300 μm) was recombined with fresh embryonic mesenchyme and grown for another 1–2 months, whereas the remainder was processed for histological analyses. Serial transplantation was performed up to five rounds for the *Nkx3.1*$^{+/-}$; *Pten*$^{+/-}$ mutants, whereas the wild-type tissue recombinants were only capable of growth for two to three rounds, as reported previously (9).

For androgen ablation studies, mice were surgically castrated by bilateral removal of the testis and epididymus. Mice were analyzed at 4 days after castration for measurement of apoptotic index or at 3 months after castration for analysis of the prostatic phenotype; the efficacy of androgen depletion was confirmed by measurement of serum levels of testosterone. Experimental groups were compared with age- and genotype-matched controls that were subjected to surgery but were not castrated (mock-castrated mice).

Results and Discussion

Neoplastic Progression of *Nkx3.1*$^{+/-}$; *Pten*$^{+/-}$ PIN Lesions in a Serial Transplantation Assay. In previous studies, we observed that *Nkx3.1*$^{+/-}$; *Pten*$^{+/-}$ compound mutant mice develop high-grade PIN by 6 months of age (10). [In this work, we define high-grade PIN as having the histopathological features of PIN III and IV, corresponding to foci of atypical epithelial cells that fill the lumen of the ducts, with solid, cribriform, or tufting architecture, as well as severe nuclear pleomorphism and hyperchromasia (16).] Although the high-grade PIN lesions in *Nkx3.1*$^{+/-}$; *Pten*$^{+/-}$ mice have many features in common with equivalent stages of human prostate cancer, including a high proliferative index and extensive neovascularization (10), their malignant potential has remained unresolved. To address this issue, we have used a serial tissue recombination/transplantation assay to investigate the potential neoplastic progression of these high-grade PIN lesions from *Nkx3.1*$^{+/-}$; *Pten*$^{+/-}$ mice (Fig. 1). We previously used this approach to show that low-grade PIN lesions from *Nkx3.1* mutants can undergo progressive histopathological changes after serial transplantation in nude mice (9).

We found that the histopathology of first-round tissue recombinants made from the prostatic epithelium of *Nkx3.1*$^{+/-}$; *Pten*$^{+/-}$ mice strongly resembled that of the PIN lesions from which they were derived ($n = 12$), similar to our previous observations using *Nkx3.1* tissue recombinants (9). The first-round *Nkx3.1*$^{+/-}$; *Pten*$^{+/-}$ tissue recombinants displayed (*a*) large foci of atypical epithelial cells that filled the prostatic ducts; (*b*) an irregular but continuous fibromuscular sheath, as detected by expression of smooth muscle α-actin; (*c*) high-level expression of AR; (*d*) heterogeneous expression of E-cadherin in lumenal cells; (*e*) robust expression of activated Akt kinase (*p*-Akt), which is consistent with inactivation of *Pten*; and (*f*) irregular distribution of p63-positive basal cells (Fig. 1, *A*, *C*, *E*, *G*, and *I* and data not shown). These histopathological features are characteristic of high-grade PIN in *Nkx3.1*$^{+/-}$; *Pten*$^{+/-}$ mice (10), as well as human PIN (1).

After up to five rounds of serial tissue transplantation, the *Nkx3.1*$^{+/-}$; *Pten*$^{+/-}$ tissue recombinants displayed a striking neoplastic progression (Fig. 1, *B*, *D*, *F*, *H*, and *J*). Whereas the first-round tissue grafts were only loosely associated with the host kidney tissue, the subsequent rounds of serial transplants ($n = 8$) displayed extensive stromal infiltration between the host kidney glomeruli (Fig. 1, *C* and *D*). Notably, these invasive stromal cells were derived from genetically wild-type urogenital mesenchyme in the tissue recombinants; similar but less severe stromal defects were observed in the *Nkx3.1* serial transplants (9). Moreover, in contrast to the extensively hyperplastic atypical epithelium that characterized the parental high-grade PIN lesions and the first-round tissue recombinants, the serial transplants formed small well-differentiated ducts with a single epithelial layer that coexpressed markers of lumenal (E-cadherin) and

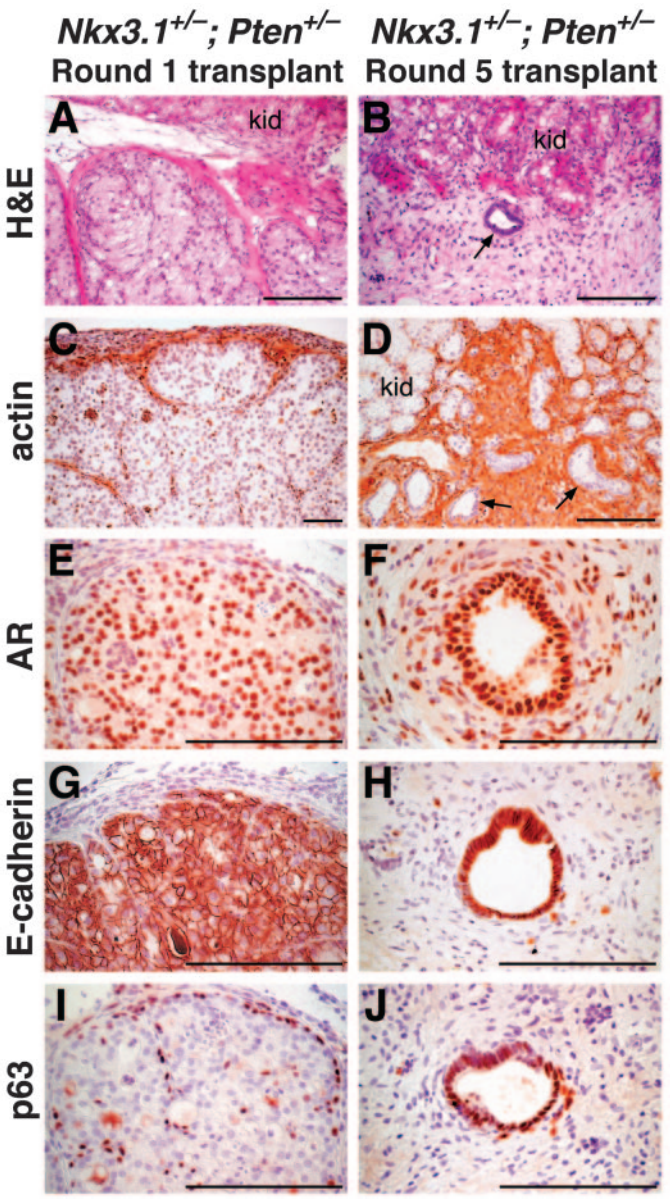

Fig. 1. Neoplastic progression of high-grade PIN lesions from *Nkx3.1*$^{+/-}$; *Pten*$^{+/-}$ mutant mice after serial transplantation in tissue recombinants. Sections of tissue recombinants generated with prostatic epithelium from an 8 month *Nkx3.1*$^{+/-}$; *Pten*$^{+/-}$ mutant after growth in nude male hosts for one round (*A*, *C*, *E*, *G*, and *I*) or after five rounds (*B*, *D*, *F*, *H*, and *J*). *A* and *B*, H&E staining (H&E) shows that in the round 1 transplant, the tissue recombinant is only loosely associated the host kidney (*kid*), whereas in the round 5 transplant the small duct-like structures (*arrow*) are juxtaposed to the host kidney. *C* and *D*, immunostaining with antismooth muscle actin shows an intact fibromuscular sheath in the round 1 transplant, compared with the round 5 transplant in which the stroma invades the kidney glomeruli; *arrows* in *D* indicate prostatic ducts. *E* and *F*, immunostaining for AR shows positive staining of epithelial cells in round 1 and round 5 transplants. *G* and *H*, immunostaining for E-cadherin in the PIN lesion of the round 1 transplant, and in the single-layered duct of the round 5 transplant. *I* and *J*, in the round 1 transplant, p63 immunostaining shows an expected distribution in basal layer surrounding the PIN regions, whereas the single-layered duct stains positively for p63 in the round 5 transplant. *Scale bars* correspond to 100 μm.

basal (p63) cells, as well as AR and *p*-Akt (Fig. 1, *F*, *H*, *J*, and *L* and data not shown). Notably, these features are often associated with well-differentiated adenocarcinoma in humans (1).

The neoplastic progression of high-grade PIN lesions from *Nkx3.1*$^{+/-}$; *Pten*$^{+/-}$ mice in serial transplants confirms their malignant potential and highlights the similarities of these lesions to human adenocarcinoma. Furthermore, together with our previous findings for *Nkx3.1* mutant mice (9), these results establish this serial transplantation assay as a valuable approach for evaluating the malignant potential of precancerous lesions from mouse models of carcinogenesis for the prostate and possibly other tissues.

Invasive Prostate Adenocarcinoma in Aged *Nkx3.1*$^{+/-}$; *Pten*$^{+/-}$ Mice. Although the prostatic phenotype of the *Nkx3.1*$^{+/-}$; *Pten*$^{+/-}$ mice rarely progresses beyond high-grade PIN by 6 months of age (10), we have now found that *Nkx3.1*$^{+/-}$; *Pten*$^{+/-}$ mice are highly prone to invasive prostate adenocarcinoma after 12 months of age (Fig. 2). (The experiments described here compare *Nkx3.1*$^{+/-}$; *Pten*$^{+/-}$ compound heterozygotes with *Nkx3.1*$^{+/+}$; *Pten*$^{+/+}$ wild-type littermate controls; the analysis of the complete set of genotypic combinations will be described in detail elsewhere).[5] These aged *Nkx3.1*$^{+/-}$; *Pten*$^{+/-}$ mice develop large masses of epithelial cells that engorge the prostatic lobes and display evidence of local microinvasion into the surrounding stroma as well as a marked inflammatory response (Fig. 2, *B* and *E*; data not shown). Despite the greatly enlarged stroma, the smooth muscle layer surrounding the epithelium is thin and discontinuous (Fig. 2*H*). The epithelial cells were highly proliferative and expressed high levels of AR and *p*-Akt, whereas expression of E-cadherin is heterogeneous and often absent (Fig. 2, *K*, *N*, *Q*, and *W*); however, there is no detectable expression of the neuroendocrine marker synaptophysin (data not shown). Interestingly, p63-expressing cells were not only confined to the rim of the cancer regions but were also scattered throughout the tumor masses (Fig. 2*T*). Taken together, these findings indicate that aged *Nkx3.1*$^{+/-}$; *Pten*$^{+/-}$ mice develop adenocarcinoma, which recapitulates many of the histopathological features of human prostate cancer.

We also observed that the prostate phenotype of the *Nkx3.1*$^{+/-}$; *Pten*$^{+/-}$ mice is considerably more severe in the DLP than in the anterior or ventral lobes; in particular, invasive carcinoma was less frequently observed in the anterior lobes than in the DLP (data not shown). This differential susceptibility of the DLP to prostate cancer in *Nkx3.1*$^{+/-}$; *Pten*$^{+/-}$ mice is notable because embryological comparisons of mouse and human prostate development have suggested that the mouse DLP most closely resembles the peripheral zone (discussed in Ref. 3), where most human prostate cancer occurs.

Finally, the progression from high-grade PIN to adenocarcinoma in *Nkx3.1*$^{+/-}$; *Pten*$^{+/-}$ mice is markedly dependent on aging. We did not observe any cases of invasive carcinoma in *Nkx3.1*$^{+/-}$; *Pten*$^{+/-}$ mice at <1 year of age, whereas older mice developed microinvasion and/or overt carcinoma in 84% of the cases (Table 1 and data not shown). Given the significance of aging for prostate carcinogenesis in humans (2), these *Nkx3.1*$^{+/-}$; *Pten*$^{+/-}$ mice may provide an ideal model system to elucidate the molecular pathways that link aging to prostate carcinogenesis.

High-Grade PIN Lesions in *Nkx3.1*$^{+/-}$; *Pten*$^{+/-}$ Mutants Are Resistant to Androgen Ablation. Given the clinical significance of the transition to androgen-independent cancer in humans, we investigated the consequences of androgen ablation on the prostate phenotype of *Nkx3.1*$^{+/-}$; *Pten*$^{+/-}$ mice. For this purpose, we castrated *Nkx3.1*$^{+/-}$; *Pten*$^{+/-}$ mutants or littermate controls at 6 months of age,

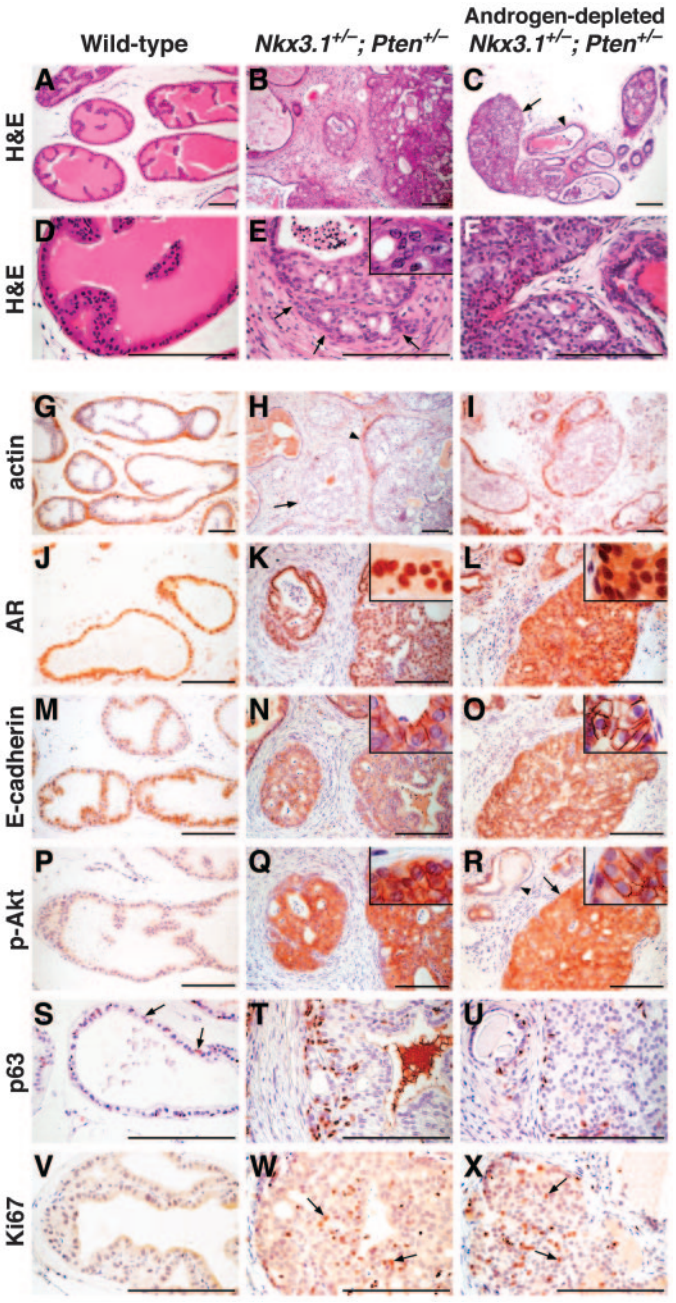

Fig. 2. Adenocarcinoma and androgen independence in *Nkx3.1*$^{+/-}$; *Pten*$^{+/-}$ mutant mice. Sections from the dorsolateral prostate from a wild-type control at 13 months (*A*, *D*, *G*, *J*, *M*, *P*, *S*, and *V*), an *Nkx3.1*$^{+/-}$; *Pten*$^{+/-}$ mutant at 15 months (*B*, *E*, *H*, *K*, *N*, *Q*, *T*, and *W*), and an *Nkx3.1*$^{+/-}$; *Pten*$^{+/-}$ mutant at 9 months, after surgical castration at 6 months of age (*C*, *F*, *I*, *L*, *O*, *R*, *U*, and *X*). *A–F*, H&E analyses. *A* and *D*, normal prostate. *B* and *E*, adenocarcinoma with local microinvasion (*arrows* in *E*); note the large mass of epithelial cells and enlarged stroma. *Inset* in *E* shows abnormal cytology in region of microinvasion. *C* and *F*, an androgen-independent high-grade PIN lesion (*arrow* in *C*) in proximity to involuted ducts (*arrowhead*). *G–U*, immunohistochemical analyses. *G–I*, immunostaining for smooth muscle actin; in *H* and *I*, note that the attenuation of actin-positive cells (*arrow* in *H*) and disorganization of the fibromuscular sheath (*arrowhead*). *J–L*, AR immunostaining is primarily localized to the nucleus in normal and *Nkx3.1*$^{+/-}$; *Pten*$^{+/-}$ mice (*inset* in *K*) but predominantly to the cytoplasm in androgen-depleted mice (*inset* in *L*). *M–O*, immunostaining for E-cadherin shows heterogeneous staining of epithelial cells in invasive regions (*N*); *insets* in *N* and *O* show cell-surface localization of staining. *P–R*, immunostaining for *p*-Akt is robust in regions of carcinoma (*Q*) and in the androgen-independent high-grade PIN lesions (*arrow* in *R*) but is heterogeneous in the adjacent involuted ducts (*arrowhead*); *insets* in *Q* and *R* show cell-surface localization of staining. *S–U*, immunostaining for p63 reveals positive cells interspersed in the invasive lesion (*T*) in contrast with normal prostate and PIN lesions where the p63-positive cells are localized to the basal layer (*S* and *U*). *V–X*, Ki67 staining shows a high proliferative index in regions of carcinoma (*W*), as well as in an androgen-independent PIN lesion (*X*). *Scale bars* correspond to 100 μm.

[5] H. Gao, W. A. Banach-Petrosky, K. D. Economides, X. Sun, M. Kim, J. P. Gregg, A. D. Borowski, R. D. Cardiff, M. M. Shen, and C. Abate-Shen, Cooperativity of Nkx3.1, PTEN, and P27 in Prostate Carcinogenesis, manuscript in preparation.

Table 1 *Incidence of adenocarcinoma and metastases in aged Nkx3.1; Pten mice*

Genotype[a]	Incidence of high-grade PIN with invasion[b]	Incidence of metastases to lymph nodes[c]
Nkx3.1$^{+/+}$; *Pten*$^{+/+}$	0/6	0/3
Nkx3.1$^{+/-}$; *Pten*$^{+/+}$	0/5	0/1
Nkx3.1$^{+/+}$; *Pten*$^{+/-}$	7/13 (54%)	0/4
Nkx3.1$^{+/-}$; *Pten*$^{+/-}$	22/26 (84%)	4/16 (25%)

[a] Mice were 12–15 months of age.
[b] High-grade PIN includes PIN III and IV as defined by (16).
[c] Metastases were identified by H&E staining as well as by immunohistochemistry with antisera against androgen receptor and E-cadherin.

which coincides with the onset of frequent high-grade PIN lesions (10), and analyzed them 3 months later at 9 months of age.

In contrast to wild-type mice, in which the prostate and other androgen-dependent tissues of the male urogenital system were involuted at 3 months after castration ($n = 2$; data not shown), the prostatic lobes of *Nkx3.1; Pten* compound mutants did not fully regress, despite the complete involution of other androgen-dependent tissues ($n = 8$). Instead, the prostatic lobes of androgen-depleted *Nkx3.1*$^{+/-}$; *Pten*$^{+/-}$ mutant mice contained numerous sizable high-grade PIN lesions, often adjacent to involuted ducts (Fig. 2, *C* and *F*). These high-grade PIN lesions had histopathological features resembling those from noncastrated *Nkx3.1*$^{+/-}$; *Pten*$^{+/-}$ mice, including a thin and irregular fibromuscular sheath, heterogeneous expression of E-cadherin, perturbations of the basal layer (Fig. 2, *I*, *O*, and *U*). In contrast, however, AR expression in the castrate PIN lesions was predominantly localized to the cytoplasm (Fig. 2*L*, *inset*), consistent with the predicted consequences of androgen ablation (17). Notably, the high-grade PIN lesions from the androgen-depleted mice were highly proliferative and were lacking apoptotic cells (Fig. 2*X* and data not shown). Consequently, these high-grade PIN lesions in castrated *Nkx3.1*$^{+/-}$; *Pten*$^{+/-}$ mice appear to be androgen independent.

Interestingly, we observed robust levels of membrane-localized *p*-Akt in high-grade PIN lesions from the androgen-depleted *Nkx3.1*$^{+/-}$; *Pten*$^{+/-}$ mutant mice, whereas *p*-Akt was detected at much lower levels in the adjacent involuted ducts (Fig. 2*R*). This observation is consistent with the idea that Akt signaling plays a critical role in progression to an androgen-independent phenotype, as has been suggested from cell culture studies (*e.g.,* Ref. 18).

Our findings suggest that *Nkx3.1*$^{+/-}$; *Pten*$^{+/-}$ mice can provide a valuable model for studying the transition to androgen-independent prostate cancer in humans, which is typically associated with a highly aggressive disease. However, whereas the high-grade PIN lesions of the androgen-depleted *Nkx3.1*$^{+/-}$; *Pten*$^{+/-}$ mice did not involute, they also did not display a significant phenotypic progression. It is conceivable that other genetic and epigenetic events will be required for progression to a more aggressive, androgen-independent disease in *Nkx3.1*$^{+/-}$; *Pten*$^{+/-}$ mice; one likely candidate factor is aging, which we are currently investigating in similar androgen ablation studies with older *Nkx3.1*$^{+/-}$; *Pten*$^{+/-}$ mutant mice.

Detection of Lymph Node Metastases. In addition to the formation of adenocarcinoma, aged *Nkx3.1*$^{+/-}$; *Pten*$^{+/-}$ mutant mice also frequently display metastases to the iliac lymph nodes. These metastases are histologically apparent as prostatic-like ducts that are often filled with secretory material (Fig. 3*A*). They are generally located in the subcapsular region of the lymph node and are all highly positive for AR (Fig. 3, *A* and *B*). The occurrence of these metastases is tightly correlated with the severity of the prostatic phenotype such that these metastases were only detected in aged *Nkx3.1*$^{+/-}$; *Pten*$^{+/-}$ mutant mice (older than 12 months) and not in younger mice or in mice of genotypes that did not develop invasive carcinoma (Table 1). Notably, the metastatic lesions from the *Nkx3.1*$^{+/-}$; *Pten*$^{+/-}$ mice bear a striking resemblance to lymph node metastases found in human patients with advanced prostate cancer (Fig. 3, *C* and *D*).

Importantly, the *Nkx3.1*$^{+/-}$; *Pten*$^{+/-}$ lymph node metastases express prostatic secretory proteins that are detectable using an antibody against DLP secretory proteins (Fig. 3*E*), confirming their prostatic origin. They also share several features in common with the prostate carcinoma lesions from which they are presumably derived because they are comprised of epithelial cells expressing cytokeratins, with heterogeneous staining for E-cadherin and *p*-Akt (Fig. 3, *F*, *G*, and *H*). The metastatic ducts contain both lumenal (CK8-expressing) and basal (p63-expressing) cells (Fig. 1*J*) and are therefore fairly well differentiated.

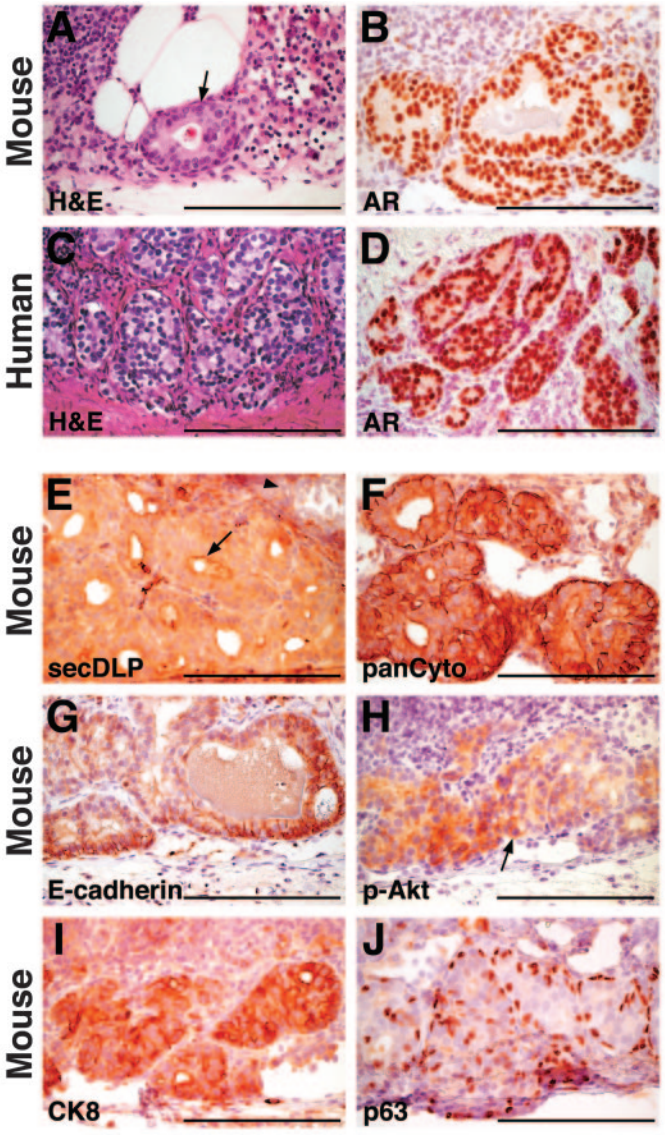

Fig. 3. Lymph node metastases in aged *Nkx3.1*$^{+/-}$; *Pten*$^{+/-}$ mutant mice. *A*, *B*, and *E–J*, sections from the iliac lymph node of the 15-month *Nkx3.1*$^{+/-}$; *Pten*$^{+/-}$ mutant whose prostatic tumor was analyzed in Fig. 2. *C* and *D*, sections from a human lymph node of a patient with a metastatic prostate adenocarcinoma that was poorly differentiated and had a Gleason score of 9. *A* and *C*, H&E staining of prostatic-like ducts in the subcapsular region of the lymph node in the mouse and human lymph nodes. *B* and *D*, immunostaining for AR in the prostatic-like ducts of both the mouse and human lymph nodes. *E*, antisera against prostatic secretions (secDLP) confirm the prostatic origin of the mouse lymph node metastases; *arrow* shows more intense staining at apical surface of lumenal cells. *F*, antisera against pan-cytokeratins (panCyto) shows that the metastases are comprised of epithelial cells. *G*, immunostaining with E-cadherin is heterogeneous. *H*, the metastatic ducts stain positively for *p*-Akt. *I* and *J*, immunostaining of metastatic ducts for lumenal (CK8, *I*) and basal (p63, *J*) cell markers shows that they are well differentiated. Scale bars correspond to 100 μm.

Taken together, these observations provide strong evidence that *Nkx3.1*$^{+/-}$*; Pten*$^{+/-}$ mutant mice provide an accurate model for human prostate adenocarcinoma. Although our findings demonstrate the frequent occurrence of metastatic prostate cancer in aged *Nkx3.1*$^{+/-}$*; Pten*$^{+/-}$ mice, we have not yet observed overt metastases to tissues other than lymph nodes such as lung, liver, or bone. However, we cannot exclude the existence of metastases to other tissues because the histological and immunohistochemical methods of detection that we have used are prone to false negatives. In principle, these difficulties can be circumvented by the development of more aggressive disease models and by utilization of more effective strategies for detection of metastases such as whole-animal imaging methodologies.

Our *Nkx3.1; Pten* loss-of-function mouse model provides a useful contrast with transgenic models that are based on targeted expression of SV40 viral oncogenes to the prostate using the probasin promoter (reviewed in Ref. 4). Notably, these transgenic gain-of-function models display severe histopathological phenotypes accompanied by metastases to the lungs and liver and less often to the bone and can also develop androgen-independent disease after castration (19–21). One key difference is that at least some of these transgenic models are prone to develop neuroendocrine tumors rather than adenocarcinoma (21, 22); another distinction is that the transition to androgen independence in these models may be mechanistically dissimilar because the probasin promoter is itself androgen sensitive. Nonetheless, these transgenic models recapitulate many of the molecular features of human prostate carcinogenesis and represent an important complement to *Nkx3.1; Pten* loss-of-function mice.

In summary, our findings demonstrate that *Nkx3.1*$^{+/-}$*; Pten*$^{+/-}$ mice develop several key features of advanced stages of prostate cancer, including invasiveness, the potential for androgen independence and for metastases, and a critical dependence on aging for disease progression. Although the *Nkx3.1*$^{+/-}$*; Pten*$^{+/-}$ mice do not yet recapitulate all aspects of advanced prostate cancer, the continued analysis and refinement of this model may reveal additional points of similarity to human cancer. Finally, we anticipate that next-generation mouse models that incorporate conditional gene targeting coupled with imaging approaches should significantly enhance the applicability of mouse models for the study of advanced prostate cancer.

Acknowledgments

We thank Hodan Ali for excellent technical assistance in mouse husbandry and genotyping and Judy Walls for histopathology.

References

1. DeMarzo, A., Nelson, W. G., Isaacs, W. G., and Epstein, J. I. Pathology and molecular aspects of prostate cancer. Lancet, *361:* 955–964, 2003.
2. Isaacs, W., De Marzo, A., and Nelson, W. G. Focus on prostate cancer. Cancer Cell, *2:* 113–116, 2002.
3. Abate-Shen, C., and Shen, M. M. Molecular genetics of prostate cancer. Genes Dev., *14:* 2410–2434, 2000.
4. Abate-Shen, C., and Shen, M. M. Mouse models of prostate carcinogenesis. Trends Genet., *18:* S1–S5, 2002.
5. Dong, J. T. Chromosomal deletions and tumor suppressor genes in prostate cancer. Cancer Metastasis Rev., *20:* 173–193, 2001.
6. Voeller, H. J., Augustus, M., Madike, V., Bova, G. S., Carter, K. C., and Gelmann, E. P. Coding region of NKX3.1, a prostate-specific homeobox gene on 8p21, is not mutated in human prostate cancers. Cancer Res., *57:* 4455–4459, 1997.
7. Bowen, C., Bubendorf, L., Voeller, H. J., Slack, R., Willi, N., Sauter, G., Gasser, T. C., Koivisto, P., Lack, E. E., Kononen, J., Kallioniemi, O. P., and Gelmann, E. P. Loss of NKX3.1 expression in human prostate cancers correlates with tumor progression. Cancer Res., *60:* 6111–6115, 2000.
8. Bhatia-Gaur, R., Donjacour, A. A., Sciavolino, P. J., Kim, M., Desai, N., Young, P., Norton, C. R., Gridley, T., Cardiff, R. D., Cunha, G. R., Abate-Shen, C., and Shen, M. M. Roles for Nkx3.1 in prostate development and cancer. Genes Dev., *13:* 966–977, 1999.
9. Kim, M. J., Bhatia-Gaur, R., Banach-Petrosky, W. A., Desai, N., Wang, Y., Hayward, S. W., Cunha, G. R., Cardiff, R. D., Shen, M. M., and Abate-Shen, C. Nkx3.1 mutant mice recapitulate early stages of prostate carcinogenesis. Cancer Res., *62:* 2999–3004, 2002.
10. Kim, M. J., Cardiff, R. D., Desai, N., Banach-Petrosky, W. A., Parsons, R., Shen, M. M., and Abate-Shen, C. Cooperativity of Nkx3.1 and Pten loss of function in a mouse model of prostate carcinogenesis. Proc. Natl. Acad. Sci. USA, *99:* 2884–2889, 2002.
11. McMenamin, M. E., Soung, P., Perera, S., Kaplan, I., Loda, M., and Sellers, W. R. Loss of PTEN expression in paraffin-embedded primary prostate cancer correlates with high Gleason score and advanced stage. Cancer Res., *59:* 4291–4296, 1999.
12. Di Cristofano, A., and Pandolfi, P. P. The multiple roles of PTEN in tumor suppression. Cell, *100:* 387–390, 2000.
13. Vivanco, I., and Sawyers, C. L. The phosphatidylinositol 3-kinase AKT pathway in human cancer. Nat. Rev. Cancer, *2:* 489–501, 2002.
14. Di Cristofano, A., De Acetis, M., Koff, A., Cordon-Cardo, C., and Pandolfi, P. P. Pten and p27KIP1 cooperate in prostate cancer tumor suppression in the mouse. Nat. Genet., *27:* 222–224, 2001.
15. Podsypanina, K., Ellenson, L. H., Nemes, A., Gu, J., Tamura, M., Yamada, K. M., Cordon-Cardo, C., Catoretti, G., Fisher, P. E., and Parsons, R. Mutation of Pten/Mmac1 in mice causes neoplasia in multiple organ systems. Proc. Natl. Acad. Sci. USA, *96:* 1563–1568, 1999.
16. Park, J. H., Walls, J. E., Galvez, J. J., Kim, M., Abate-Shen, C., Shen, M. M., and Cardiff, R. D. Prostatic intraepithelial neoplasia in genetically engineered mice. Am. J. Pathol., *161:* 727–735, 2002.
17. Gelmann, E. P. Molecular biology of the androgen receptor. J. Clin. Oncol., *20:* 3001–3015, 2002.
18. Li, P., Nicosia, S. V., and Bai, W. Antagonism between PTEN/MMAC1/TEP-1 and androgen receptor in growth and apoptosis of prostatic cancer cells. J. Biol. Chem., *276:* 20444–20450, 2001.
19. Gingrich, J. R., Barrios, R. J., Morton, R. A., Boyce, B. F., DeMayo, F. J., Finegold, M. J., Angelopoulou, R., Rosen, J. M., and Greenberg, N. M. Metastatic prostate cancer in a transgenic mouse. Cancer Res., *56:* 4096–4102, 1996.
20. Gingrich, J. R., Barrios, R. J., Kattan, M. W., Nahm, H. S., Finegold, M. J., and Greenberg, N. M. Androgen-independent prostate cancer progression in the TRAMP model. Cancer Res., *57:* 4687–4691, 1997.
21. Masumori, N., Thomas, T. Z., Chaurand, P., Case, T., Paul, M., Kasper, S., Caprioli, R. M., Tsukamoto, T., Shappell, S. B., and Matusik, R. J. A probasin-large T antigen transgenic mouse line develops prostate adenocarcinoma and neuroendocrine carcinoma with metastatic potential. Cancer Res., *61:* 2239–2249, 2001.
22. Kaplan-Lefko, P. J., Chen, T. M., Ittmann, M. M., Barrios, R. J., Ayala, G. E., Huss, W. J., Maddison, L. A., Foster, B. A., and Greenberg, N. M. Pathobiology of autochthonous prostate cancer in a pre-clinical transgenic mouse model. Prostate, *55:* 219–237, 2003.